PROCEEDINGS, Thirty-Seventh Workshop on Geothermal Reservoir Engineering
Stanford University, Stanford, California, January 30 - February 1, 2012
SGP-TR-194

TOWARDS DEVELOPING A CALIBRATED EGS EXPLORATION METHODOLOGY USING THE DIXIE VALLEY GEOTHERMAL SYSTEM, NEVADA

Joe Iovenitti[1], David Blackwell[2], Jon Sainsbury[1], Ileana Tibuleac[3], Al Waibel[4], Trenton Cladouhos[5], Robert Karlin[6], Ed Isaaks[7], Matthew Clyne[1], Fletcher Hank Ibser[8], Owen Callahan[5], B. Mack Kennedy[9], Philip Wannamaker[10]

[1]AltaRock Energy Inc., Sausalito, California 94596, USA
[2]Southern Methodist University, Dept. of Earth Sciences, Dallas, Texas 75275, USA
[3]University of Nevada Reno, Nevada Seismological laboratory, Reno, Nevada 89557, USA
[4]Columbia Geoscience, Hillsboro, Oregon 97124, USA
[5]AltaRock Energy Inc., Seattle, Washington 98103, USA
[6]University of Nevada Reno, Department of Geology, Reno, Nevada 89557, USA
[7]Isaaks & Company, Redwood City, California 94062, USA
[8]University of California, Berkeley, Department of Statistics, Berkeley, California 94720, USA
[9]Lawrence Berkeley National Laboratory, Earth Science Division, Berkeley, California 94720, USA
[10]Univeristy of Utah, Energy and Geoscience Institute, Salt Lake City, Utah 84108, USA

jiovenitti@altarockenergy.com

ABSTRACT

A calibrated Engineered Geothermal System (EGS) exploration methodology is being developed using the Dixie Valley Geothermal Wellfield (DVGW) and its surroundings in central Nevada as a laboratory test site. The DVGW was chosen because in the public domain, it is a highly characterized Basin and Range site with considerable geoscience and well data.

This paper presents the qualitative and quantitative geoscience assessment used to develop a baseline geothermal system conceptual model based on existing available data. This assessment includes the integration of geophysical, geological, and geochemical data sets coupled with subject matter expertise (SME), and geostatistical exploratory data analysis (EDA). The baseline model is then used to generate paired EGS favorability and trust maps from the integrated evaluation of the following three principal EGS parameters of interest: temperature, rock type, and stress, at depths from +1km to -4km above sea level. Trust maps provide a data reliability indicator. When coupled, the two maps provide an EGS favorability determination, a SME evaluation of the reliability of the underlying data used in this determination, and an indication where additional data may be required. For example, an area could be mapped as being highly favorable but the underlying supporting data used in the favorability determination is of low reliability.

Statistical relationships among select geoscience parameters are also described. In part, these relationships have provided insight into which geoscience parameters may be used as a predictor of subsurface temperature and rock type. Calibration of the exploration assessment methodology is based on the cross-correlation of the aforementioned findings with known well results.

This paper builds upon the progress report provided in Iovenitti et al. (2011a, 2011b) and presents additional details of the geoscience assessment, EDA, and baseline EGS favorability/trust maps. Finally, much of the data and the approach presented herein are also applicable to the exploration/development of the hydrothermal component of the geothermal system.

INTRODUCTION

This project is being conducted under American Recovery and Reinvestment Act (ARRA) funding through the U.S. Department of Energy (DOE) and AltaRock Energy Inc. to develop a calibrated Engineered Geothermal System (EGS) exploration methodology (DOE contract no. DE-EE0002778). The project consists of five major tasks (1) reviewing and assessing the existing public domain and limited private sector (referred to as baseline) data made available by Terra-Gen Power, LLC. for the Dixie Valley Geothermal System (Figure 1); (2) developing and populating a Geographic Information System (GIS)-database; (3) developing a baseline geothermal conceptual model, evaluating geostatistical relationships between the various geoscience data sets, and generating baseline EGS favorability/trust map pairs from +1km to -4km above sea level (asl) focused on identifying EGS drilling targets based on three key EGS parameters of interest: temperature,

rock type, and stress; (4) collecting new gravity, seismic, magnetotellurics (MT), geologic, and geochemical data to fill in data gaps and improve model resolution; and (5) updating the GIS-database for the newly acquired data and repeating Task 3 incorporating the baseline and new data to generate an enhanced geothermal system conceptual model, EDA, and EGS favorability/trust map pairs. In preparing the baseline EGS favorability maps, it was recognized that they alone were insufficient to adequately reflect the validity of the favorability determination since they provided no indication as to the reliability of the underlying data set. As such, paired favorability and trust maps were developed to reflect the dual requirement of EGS favorability and data reliability.

The Dixie Valley geothermal area was chosen for the development of a calibrated EGS exploration methodology project because it is considered among the best characterized Basin and Range (B&R) geothermal system in the public domain with a considerable amount of geoscience data and known well results. Over 60 MW is being generated from the Dixie Valley Producing Field (DVPF, Figure 1). This geothermal system also has the highest bottomhole temperature in any geothermal well in the B&R, 285°C at 3000m in well 36-14, in the Dixie Valley Power Partners (DVPP) portion of the wellfield (Figure 1). Additionally, the Dixie Valley Geothermal Wellfield (DVGW) lies within the greater Dixie Valley Geothermal District, which is defined as a region encompassing multiple occurrences of geothermal cells/systems (Figure 2; Waibel, 1987, 2011; Iovenitti et al., 2011a).

The Project Area is 50km by 50 km roughly centered on the DVPF (Figure 1). The size of the project area was primarily dictated by the requirement for high-resolution geophysical data at depths of -4 to -5km asl.

For calibration purposes, we have focused our effort on the DVGW consisting of approximately 30 deep wells (Figure 1). Lithologic data was available for 22 wells, while thermal data was more limited and consisted of bottom hole temperature (BHT) measurements for 26 wells, temperature-depth profiles for 10 wells, and 9 temperature gradient holes. Additionally, a significant amount of geoscience data is available in the DVGW including geology, gravity and magnetic data and associated models, MT modeled arrays, seismic reflection profiles, seismic velocity models, and geochemical data from wells, fumaroles, and springs.

GEOLOGIC SETTING

The Dixie Valley Geothermal System, as reported by Blackwell et al., (2005), lies within (1) the Central Nevada Seismic Belt, a zone of NNE-trending focused contemporary seismicity, (2) the Battle Mountain Heat Flow high, (3) a region adjacent to a major structural discontinuity separating thicker continental crust to-the-east from thinner accreted terranes to-the-west, and (4) the lowest topographical valley in northern Nevada (Figure 3).

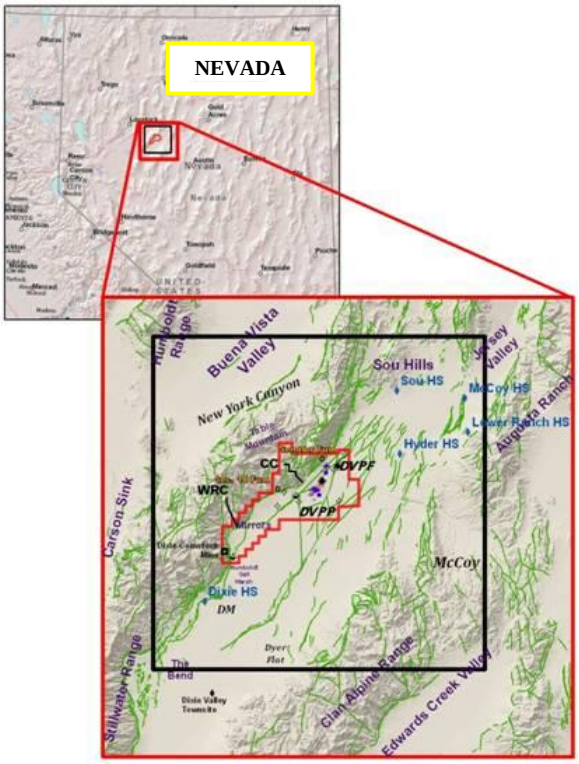

Figure 1: EGS Exploration Methodology Project Area (black square is 50km by 50km). The Dixie Valley Geothermal Wellfield (DVGW, the project calibration area), is outlined in red. Major known and inferred faulting is shown in green. The figures are after Blackwell et al. (2005).

The general stratigraphy of the area exposed in the Stillwater Range consists of allochthonous thrust plates of Triassic and Jurassic meta-sediments and Jurassic mafic igneous rocks that were intruded by late Cretaceous granodiorite and overlain by mid-Cenozoic volcanic rocks (Speed, 1976; Waibel, 1987). Within the adjacent Dixie Valley, the basement assemblage and overlying volcanics are in turn overlain by basin-fill sediments deposited during extensional events (Waibel, 1987). The stratigraphic units exposed in the area and intersected by geothermal wells have been sub-divided in this

assessment from oldest to youngest as follows (1) Triassic meta-sediments (Tr); (2) Jurassic mafic rocks also referred to as the Humboldt Igneous Group and the Humboldt Lopolith (Jz); (3) Jurassic Boyer Ranch quartzite (Jbr); (4) Cretaceous granodiorite (Kgr); (5) Oligocene silicic volcanics (Tv); (6) Miocene basalt (Tmb); and (7) late-Cenozoic basin-filling sediments (QTbf).

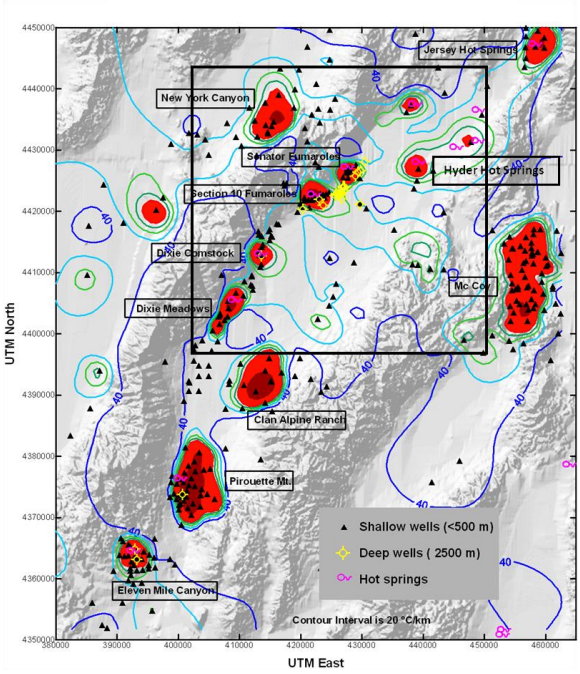

Figure 2: Shallow thermal anomalies and shallow and deep well locations in the Dixie Valley area. Contours in the ranges are diagrammatic and contour intervals are (20 °C/km). From (120 – 250 °C/km) the contours are a red fill and from (500°C/km), the contours are a dark red fill. Well gradient locations are shown as black triangles for shallow wells (<~500m) and yellow circles for wells >500m. The EGS Exploration Methodology Project Area is presented as a black square. The figure and caption are after Blackwell et al. (2005, 2007).

The relevant structural history with respect to this investigation began in the Cenozoic which was dominated by a period of E-W extension expressed by a series of N-trending normal faults, followed by WNW-ESE extension around 8Ma continuing to the present time and expressed as NNE-trending normal faults (Waibel, 1987, 2011). The N–trending structures are evident in the state of Nevada geologic map (Stewart and Carlson, 1977) and relocated natural and induced seismicity map for the greater Dixie Valley region for the period, 1900-2010, (Iovenitti et al., 2011a, 2011b).

The major range-bounding fault transecting the Project Area, the Dixie Valley Fault, is one of the most well-known normal faults in the B&R having last ruptured at the surface during the 1954 Fairview Peak-Dixie Valley earthquake, M_s6.8 in Dixie Valley and M_s7.2 at Fairview Peak, (Caskey et al., 1996). The DVPF (Figure 1) lies within a zone referred to as the Stillwater Seismic Gap which occurs south of the 1915 Pleasant Valley and north of the 1954 Fairview Peak ruptures (Wallace and Whitney, 1984; Caskey and Wesnousky, 2000).

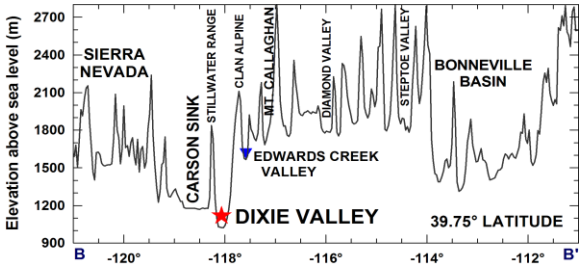

Figure 3: East–West elevation cross section through the Basin and Range from the west side of the Sierra Nevada in California to the east side of the Wasatch Mountains in Utah. Dixie Valley (red star) is the lowest point on the cross section. The figure is from Blackwell et al. (2005).

Early structural models for Dixie Valley (Okaya and Thompson, 1985; Benoit, 1999) identified a single, moderately east dipping (~54°) normal fault bounding the Stillwater Range on its eastern side and supported by surface fault measurements, interpretation of seismic reflection data, and the assumption that the producing wells located a few kilometers basinward were connected to the surface scarp of the range-front fault. More recent interpretations based on wellfield, gravity, and magnetic data defined a much more complex, multi-fault setting referred to as the Dixie Valley Fault Zone (DVFZ) within the area of the wellfield. The DVFZ is a complex and steeply dipping structure (~75-80°) consisting of the range-front fault (referred to as either the Dixie Valley Fault [Benoit, 1999] or the Stillwater Fault [Hickman et al., 1998, 2000]), and at least one major piedmont fault, which is not continuously expressed at the surface, but accounts for the majority of displacement between the range and the valley (Smith and Blackwell, 2002; Blackwell et al., 2005).

PROJECT RESULTS

Using the existing public domain data, a baseline conceptual geothermal model was developed and the qualitative correlations between various geoscience data sets were determined and crosscorrelated with

known well results. These data were quantitatively assessed using Exploratory Geostatistical Data Analyses (EDA). Described below are the structural setting findings, major qualitative correlations, the quantitative EDA results, and the paired EGS favorability and trust maps.

Qualitative Correlations

Structural Findings

A baseline conceptual structural model was developed and is summarized in Figure 4. The data sets used to derive the structure map include mapping results from Page (1965) and Speed (1976), structures identified by Smith and Blackwell (2001), geophysical inferred structures including horizontal gravity gradients (Blackwell et al., 2005), faults recognized by the state of Nevada, and from the USGS Quaternary Fault and Fold Database, and relocated seismic events in the last century indicating N-trending faults, specifically along a major active structure extending from Fairview Peak and continuing into the Project Area due west of well 45-14 (Iovenitti et al., 2011b). Figure 4 represents the compilation and interpreted relationship of all known faults and inferred structures in the Project Area. The structures are all assumed to be steeply dipping with dip directions derived from stratigraphic relationships, surface measurements, and geophysics.

Analysis of the overall structural setting of the Project Area reveals that the intersection of the pre-8 Ma N-trending B&R structures (Waibel, 1987) with the current NE-trending post-8Ma B&R structures are coincident with the location of many of the shallow thermal anomalies in the Dixie Valley Geothermal District and the DVPF, the current geothermal electrical production field (Figure 4; Waibel, 2011; Iovenitti et al., 2011a, 2011b). In some cases, the older N-trending structures appear to offset NE oriented structures within the DVFZ suggesting re-activation within the current stress regime.

The structural zones at these major fault intersections along both sides of the Stillwater Range were also divided into compressional and dilatational areas based on the expected movement within discrete structural blocks in their respective quadrants (Figure 4). The model assumes the NE-trending normal faults exhibit pure normal slip, with slip vectors perpendicular from fault strike. For the N-trending faults, the major assumption is the faults exhibit strike-slip motion under the current stress regime. This same type of motion was also reported by Caskey et al. (1996) on the Fairview Peak 1954 earthquake. The zones of compression and dilatation derived from the combination of expected slip (direction) on a NE-trending fault and the expected strike-slip component on a N-trending fault. Where both vectors agree (in same directions) a zone of dilatation is inferred. Where the vectors do not agree, a zone of compression is inferred, as movement on the strike-slip fault supersedes. Also an abrupt bend in a normal fault, apparent as the piedmont fault takes a significant left-step bend in the producing field, would also infer a dilated zone at the change in strike. The extent of these compressional and dilatational areas is purely arbitrary and defined as extending about a km away from the intersection. The structural and thermal data indicate that these structural intersections play an important role in the development of dilatational zones which are also coincident with the shallow thermal anomalies and expectedly host various geothermal cells (Figure 4) within the overall Dixie Valley Geothermal District.

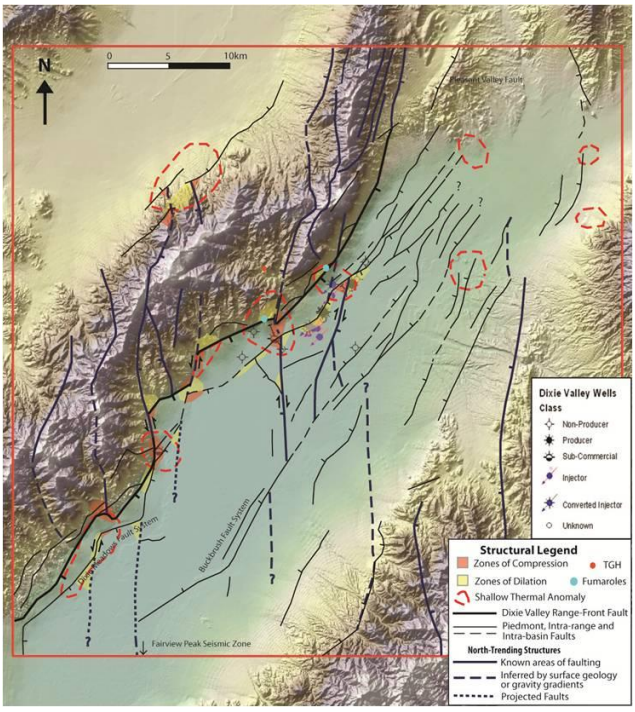

Figure 4: Correlation between shallow thermal anomalies (dashed red lines) and identified structural intersections of N to NE-trending faults (dark blue lines) in northern Dixie Valley, Nevada. Blue dots indicate the Section 10 (southwest of the producing field) and Senator fumarolic areas. Black dots indicate deep wells, while orange dots indicate the position of relatively deep temperature gradient holes. Expected zones of compression (orange shaded areas) and dilation (yellow shaded areas) occurring at the intersections of discrete structural blocks are also shown.

Table 1 correlates the structural zone type (compression, dilation, or other) with the helium R/Ra values for fumaroles and hot springs along with all baseline data for Dixie Valley deep wells subdivided into four classes: producer, sub-commercial, non-producer and injector. All available producers to this study occur in a dilation zone and these wells show a slightly elevated magmatic signature according to Kennedy and van Soest (2006). All available injectors to this study occur in a dilation or "other" structural zone. Most available non-producer/sub-commercial wells occur in a compression and/or "other" structural zone.

Role of Lithology in the Geothermal System

Rock type at elevated temperature also plays a significant role in whether a well is a producer or non-producer in a hydrothermal system and whether a well can host an EGS reservoir. Current geothermal electrical production is derived from the piedmont fault component of the DVFZ (Blackwell et al., 2005), as the geothermal reservoir lies within brittle igneous rocks including Miocene basalt and Jurassic mafic rocks that are juxtaposed against impermeable granodiorite along a steeply dipping structure (Lutz et al., 1997; Benoit, 1999; Blackwell et al., 2005; Reed, 2007).

Brittle rocks containing open-fractures are an ideal hydrothermal reservoir. When closed fractures are present in brittle rocks, the rock can be fractured through EGS.

Non-brittle rocks would not be appropriate for either a hydrothermal system or EGS. Several examples of wells completed in poor reservoir rock exist within the DVGW. The non-producers 45-14 and 66-21 have bottomhole temperatures of 196°C and 215°C, respectively, but were completed in Triassic shales, not a suitable reservoir rock (D. Benoit, pers. comm., 2011) because it does not hold a fracture, in at least the areas drilled by these wells. The northernmost producing wells, 27-33, 28-33, and 37-33, all lie within a dilatational zone, while an adjacent dry hole, 82-5, lies with a zone of compression separating the aforementioned wells from the main production area to the southwest. Hickman et al. (2000) also reported that 82-5 is completed in a narrowly defined shear zone with abundant talc alteration and low shear stress at the depth where the well was expected to encounter the producing fault zone.

Table 1: Correlation of Dixie Valley wells and associated helium R/Ra values with the structural zone type in which they occur. Geochemical data derived from Goff et al. (2001).

Structural Zone Type	Dixie Valley Well Type								Fumaroles / Hot Springs	
	Producer		Sub-Commercial		Non-Producer		Injectors			
	Well	*R/Ra*	*Well*	*R/Ra*	*Well*	*R/Ra*	*Well*	*R/Ra*	*Name*	*R/Ra*
Dilation	76A-7	**0.72**	SWL-1		45-33[a]	**0.725**	45-5		Senator	**0.662**
	82A-7	**0.691**					41-18		SE Fum	**0.855**
	73-7	**0.728**					52-18			
	73B-7	**0.659**					SWL-2			
	63-7	**0.67**					SWL-3			
	27-33	**0.728**					32-18			
	28-33	**0.681**								
	37-33	**0.727**								
	74-7	**0.694**								
Compression			36-14	**0.77**	62-23A				Dixie	**0.845**
			45-14	0.587	82-5					
Other			38-32		66-21	0.306	65-18	0.56	Sou	0.528
					62-21		27-32	0.583	Hyder	0.438
					76-28				McCoy	0.345
					53-15				Jersey	0.495

[a]Well data available to AltaRock is limited. It is unknown why this well is a non-producer.

Geoscience Correlations

A series of detailed geoscience cross-sections (perpendicular and parallel to the DVFZ) through the DVGW were constructed (Figure 5) based on public domain well data, surface and subsurface geology, available interpreted seismic reflection profiles, and geophysical surveys that inferred structures within Dixie Valley. Plate 1 presents the results of these sections perpendicular to the range-front fault as the geologic and associated thermal sections provided a basis for a correlation analysis that compared the sections with various geophysical models including MT, 2½ D gravity/magnetics, and seismic velocity models. Note that the sections are presented in a serial view looking N45°E approximately parallel to the range front fault. The analysis determined the level of correlation between four geologic and thermal sections (C-C' to F-F' [C-F]) and three associated MT arrays (N, C, S). The combined gravity and magnetics were modeled along sections C-F to infer the expected stratigraphy at depth, while velocity modeling along the same lines was based on available data (Figure 5 and Plate 1).

Iovenitti et al. (2011a, 2011b) presented the results of the geoscience correlations along section C-C'. Figure 6 presents selected geoscience correlations along section E-E'. The generalized geology section indicates the presence of the DVFZ based on surface geology, well data, and geophysical data such as the corresponding seismic reflection profile and gravity/magnetics modeling indicated in Plate 1. Important observations along section E-E' are (1) the presence of a steeply dipping low resistivity structure, roughly parallel to the range-front fault but on the footwall side, that correlates with known areas of intra-range faulting, (2) a relatively higher resistivity block associated with the geothermal reservoir in the area of the production wells in the hanging wall of the piedmont fault element of the DVFZ, (3) the similarity of the gravity-magnetic inferred lithology model with the interpreted geologic section, specifically the occurrence of the Jurassic section (Jz) defined as magnetic Jurassic mafic rocks (Jg), (4) missing Jg in the valley coincident with the major low resistivity zone to depth (Wannamaker et al., 2006, 2007) which is interpreted to reflect demagnetized Jg possibly attributed to hydrothermal alteration, (5) thermal upflow along both the range-front and piedmont faults in the DVFZ and (6) high resistivity in the Stillwater Range is not observed until about the center of the range and is interpreted as unaltered granodiorite (Kgr). The resistivity distribution under the Stillwater Range along Section E-E' suggests the presence of a hydrothermal cell in the footwall of a range-front fault component of the DVFZ in this area. Note that the dip of the faults shown on the gravity-magnetic sections is approximate and the modeled structure can easily accommodate changes in dip comparable to those shown in the geology sections.

Major correlations found throughout the sections C-F are (1) MT profiles show a high level of correlation with the interpreted structure in the geologic sections; (2) a vertical-trending low resistivity zone seen in the three MT profiles within the valley most likely reflects a major alteration zone correlating with a set of north-trending structures; (3) the gravity/magnetic profiles reflect the interpreted generalized geology, and show the magnetic signature of the Jurassic mafic rocks doesn't extend through this major north-trending intra-valley structure and is locally not present within the DVFZ; and (4) the areas of elevated temperature occur at the intersection of these earlier north-trending structures and northeast trending segments of the piedmont fault. Details about the correlations observed can be visually found in Plate 1 and are described in Iovenitti et al. (2011a, 2001b).

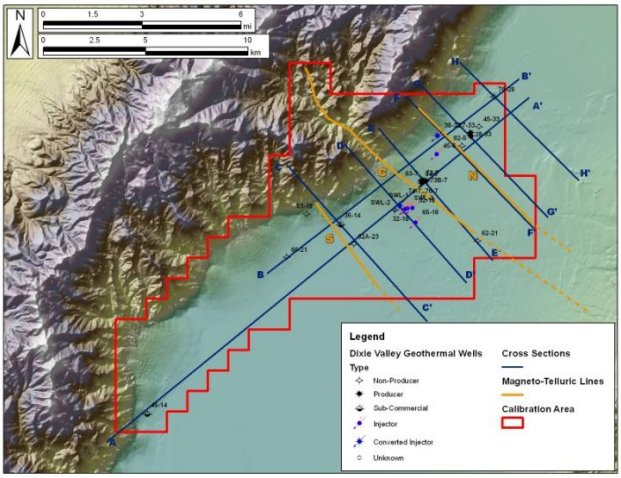

Figure 5: The Dixie Valley Geothermal Wellfield, also referred to as the Calibration Area. Location of cross-section lines, presented in Plate 1, is shown in blue. MT arrays (Wannamaker et al., 2006, 2007) are shown in orange.

Quantitative Geostatistical Analysis

EDA was applied to selected geoscience parameters, described below, to (1) quantify the qualitative geoscience correlations, (2) investigate the suggestion by Biasi et al. (2008) that seismic data correlates with temperature and rock type, (3) determine the relationship between P-wave velocity (Vp) to lithology and temperature, (4) determine the predictive power of various geoscience parameters for rock type and temperature, and (5) assist in the data generation for the EGS favorability/trust maps.

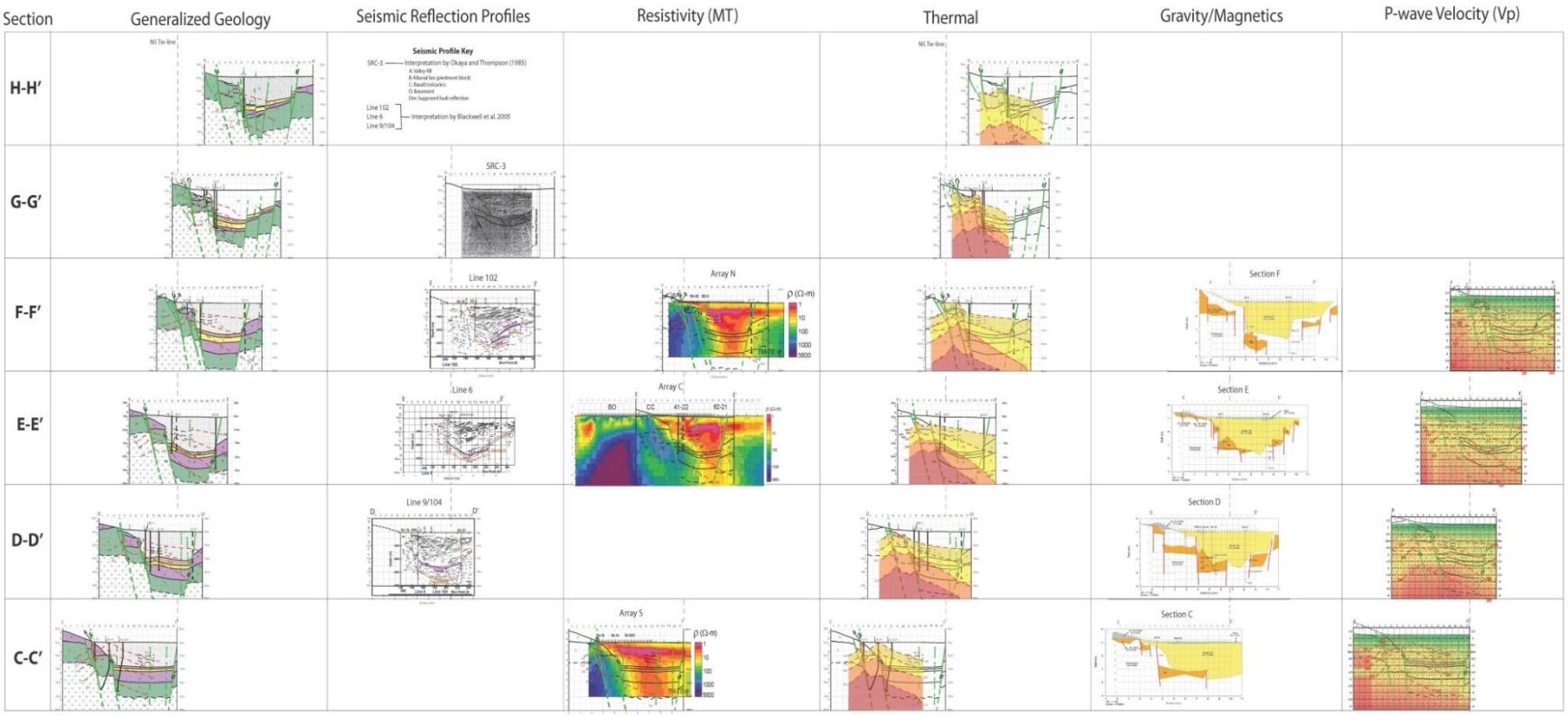

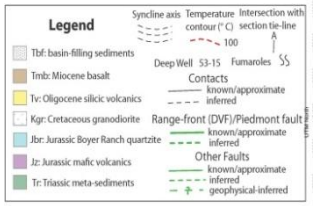

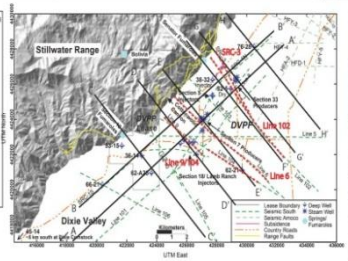

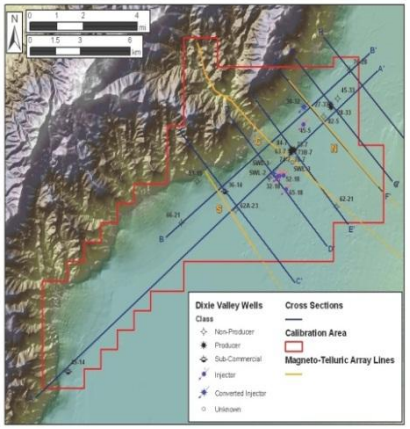

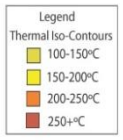

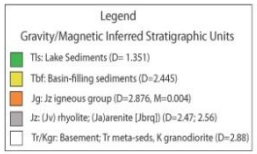

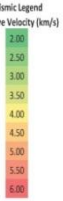

Plate 1. Correlation of Sections perpendicular to the Dixie Valley Fault Zone

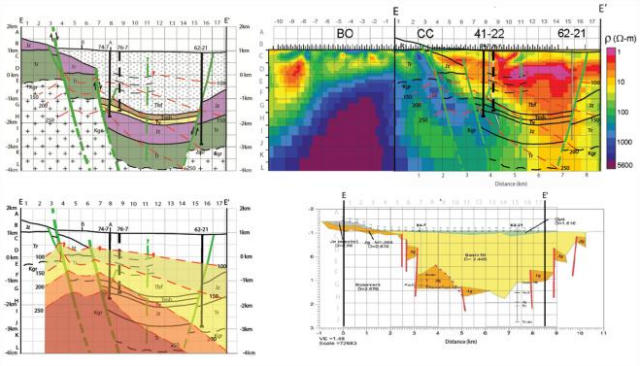

Figure 6: Correlation of the Geology, MT, Thermal, and Gravity-Magnetic Lithologic model along Section E-E', extending through the main production wells and Cottonwood Canyon (see Figure 5 for section location). Faults are in green and wells are shown as bold black lines. Note that the geology-thermal section structure and thermal elements are superimposed on the MT section.

Parameters analyzed include lithology and associated lithologic factors such as (density, fracture intensity), vertical stress, combined gravity-magnetic inferred lithology, temperature, resistivity (derived from MT), seismic parameters: Vp and Vs (S-wave velocity), and structural parameters: modeled Coulomb stress change data (CSC) and dilatation. Additional parameters were considered but not used the analysis as a result of either poor spatial resolution or limited data sets (e.g., well fluid chemistry).

The identified parameters represent the available baseline data set. The data utilized are inferred, modeled/calculated, or measured. As such, the data set is not ideal for statistical analysis. A fundamental assumption here is that while the exploration data set is statistically not ideal, and some parameters are more reliable than others, the data can be used to determine statistical significance. The validity of this assumption rests on the notion that whatever uncertainty exists in the different parameters can be thought of as a measurement error, and is at least from a practical standpoint, unbiased. Causal relationships for any statistical relationship identified herein have not been investigated. All data parameters analyzed were gridded within 500m by 500m cells generally from +1km to -4km asl for two sets of data (1) along cross-sections C-F (Figure 5 and Plate 1) and (2) with respect to wells. These data sets are referred to as sectional and well data, respectively. The latter is considered a much more reliable data set than the former.

Key geostatistical analyses performed on select geoscience parameters for the individual and combined sections C-F include (1) global (undivided per categorical groups such as lithology) linear correlation analysis; (2) multivariate analysis of various geoscience parameters per stratigraphic formation (e.g., Kgr); and (3) global domain analysis that divides the sectional data into three different geologic environments: Stillwater Range, DVFZ, and the valley. A Classification and Regression Tree (CART) to determine prediction possibilities was also conducted using sectional (combined data set) and well data..

The results of the first three types of analyses conducted are that the parameters temperature and vertical stress are independently correlated with Vp and resistivity along the sections C-F, along the sectional data with respect to stratigraphic formation, and along the sectional data with respect to geologic/geographic domains. All other correlations found are not consistent across the three analyses. The results of the CART analysis are described below.

Vp-Temperature Relationship

One objective of the geostatistical analysis was to explore if seismic data can be used to predict lithology and/or temperature. The only baseline (existing data) seismic parameter with a sufficient resolution was Vp. While a clear qualitative relationship between temperature and Vp was not found (Plate 1), the linear correlation analysis using sectional data found a correlation coefficient of over 0.90 for this relationship. Using the well data only, a linear fit was applied to all data resulting with a poor R^2-value of 0.51 (Figure 7). This linear fit was determined to be skewed by shallow Vp data, specifically modeled data at the surface (+1km asl). Also, outlier data points were found to correspond with certain wells where the associated modeled Vp data had a very low confidence (trust) value. Removing the surface data and the outlier wells (53-15, 45-14, 66-21 and 76-28, see Figure 3 for well location), found a polynomial 2-degree fit to the data with a R^2-value of 0.72 (Figure 8).

The precision of these R^2-values was estimated by the bootstrapping method with simple random sampling. Samples were taken from the data with replacement repeatedly, and for each sample the R^2-value was recalculated. Based on 10,000 samples for each R^2-value, approximate 95% confidence intervals were calculated. For the R^2-value of 0.51 found for the linear relationship between Vp and temperature, the 95% confidence interval is from 0.34 to 0.65. With

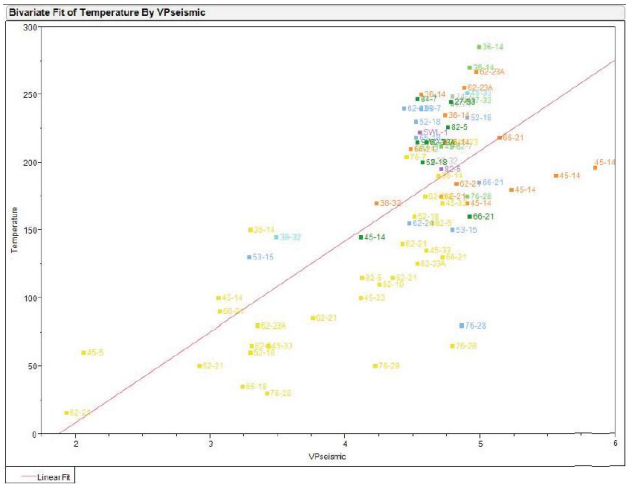

Figure 7: Correlation plot of Vp vs. Temperature using all available well data. The linear polynomial fit has a R-square value of 0.51. The data is labeled by well name and color coded by stratigraphic formations as follows: QTbf (yellow), Tmb (purple), Tv (dark green), Jz (light blue), Tr (orange), Kgr (light green) and Jbr (dark blue).

surface data and low trust value wells removed, the R^2-value of 0.72 has a 95% confidence interval of 0.54 to 0.83. These intervals are fairly wide due to the small amount of data: 76 observations for the first model and 55 for the second. However, Vp does explain a large amount of the variability in temperature, and it is reassuring that removing the modeled data with a lower trust strengthens the relationship.

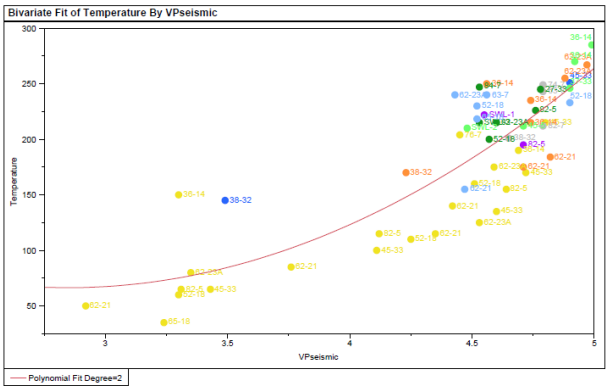

Figure 8. Correlation plot of Vp vs. Temperature using well data excluding data from +1km asl elevation and outlier wells (53-15, 66-21, 45-14 and 76-28) with a low seismic trust value. The polynomial fit has a R-square value of 0.72. See Figure 7 caption for well name and associated color code by lithology.

Multiple-Regression and Residual Analysis

In virtually all the correlation analyses conducted, a consistent relationship has been evidenced between vertical stress and Vp, and temperature and Vp. We recognized that all three of these parameters generally increase with depth and potentially that may be the reason for the observed strong correlation. For example, since vertical stress is a calculated value relying on depth and the density of rocks overlying a respective gridded cell, this parameter can be viewed as a strong indirect inference to depth. Thus, a correlation of increasing temperature with increasing vertical stress could likely be an insignificant geoscience correlation. To evaluate this postulation, a residual analysis to remove the effect of depth was conducted.

A global linear correlation (two component analysis) was performed for elevation (depth) and the selected parameters vertical stress, coulomb stress change (CSC), dilatation, temperature, Vp, Vs and resistivity using sectional data. Results indicated that linear and non-linear relationships existed between elevation and vertical stress, temperature, and Vp. These relationships were further investigated by analyzing the bivariate fit of each of the following parameters: temperature, vertical stress and Vp by elevation. High R^2- values of 0.90, 0.89, and 0.89, respectively were found indicating a strong relationship of the selected parameters with depth. Next, the residuals of this bivariate fit were calculated and the linear correlation of the remaining key variables (temperature, CSC, dilatation and resistivity) versus the residuals of Vp and vertical stress was performed with no correlation coefficient greater than 0.74 observed.

This finding is supported by a multiple (two-parameter) regression analysis of temperature and temperature predicted by the residuals of vertical stress, Vp, and Vs. The resulting R^2 value for this regression analysis was 0.19 indicating that temperature cannot be predicted by the residuals. Thus, the overall two component residual analysis indicated that depth (or elevation) is the only link between temperature and vertical stress, and Vp.

However, a multiple regression analysis of temperature vs. key geoscience parameters including elevation, vertical stress, dilatation, Vp, and resistivity using the sectional data was also performed. This multicomponent analysis indicated that (1) the combination of a variety of geoscience parameters could predict temperature with a R^2-value of 0.94 (Figure 9), and (2) there is a complex interaction between the geoscience parameters in this prediction (Figure 10). The reason for this complex interaction has not been investigated herein.

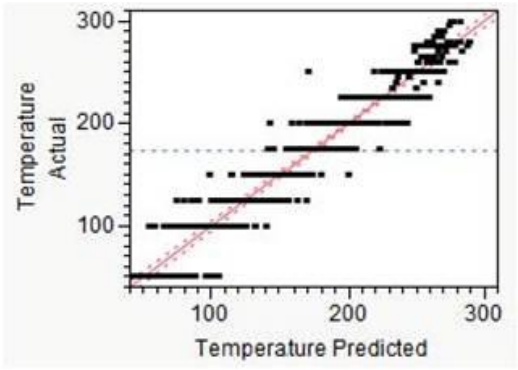

Figure 9: Actual (measured) temperature vs. predicted temperature using the following variables: elevation, resistivity, vertical stress, dilation, Vp, and Vs; R^2-value is 0.94.

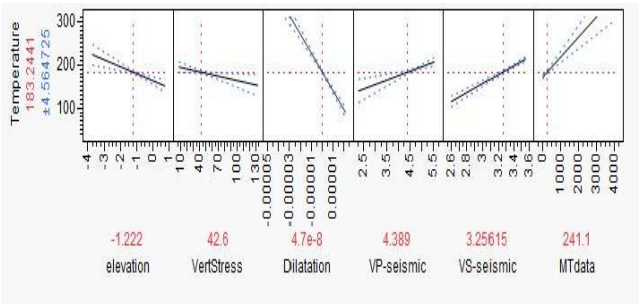

Figure 10: Example of a Predictor Profile showing the complex interactions of the indicated parameters in predicting temperature.

Classification and Regression Tree (CART)

An objective of the EDA was to define which geoscience parameters would make good predictors for favorable EGS conditions. Given that the available geoscience data and major EGS predictors (lithology, temperature, and stress) are both numerical and categorical, a statistical technique referred to as Classification and Regression Tree (CART) was utilized to predict temperature, lithology, and productive vs. non-productive wells using both the sectional and well data. The parameters showing high levels of correlation in the preceding analyses were used as response variables in the CART analysis and these include temperature, lithology type, gravity-magnetic inferred lithology, Vp, CSC, dilatation, resistivity, and vertical stress. While all potential parameters are considered as response variables, a special interest is made towards the predictive power of measurable geophysical parameters such as Vp, resistivity (from MT) and gravity-magnetic inferred lithology.

CART is a statistical method that can be used to determine the statistical relationship between a defined response variable (i.e., the parameter to be predicted, e.g., temperature), and multiple undefined explanatory variables (geoscience parameters defined above, also referred to as response variables). Lawrence and Wright (2001) describe CART as a popular form of statistical analysis that operates by recursively splitting the data until ending points, or terminal nodes, are achieved using preset criteria by analyzing all explanatory variables and determining which binary divisions of a single explanatory variable that best reduces deviance in the response variable. For each portion of the data that results from this split, the process is repeated, and continues for categorical data until homogeneous terminal nodes are reached in a hierarchical tree. In our case where numerical data is used, the split process was repeated until cross-validation determined that the deviance was no longer decreasing appreciably and thus, no more splits should be made.

Table 2 presents the results of a preliminary CART analysis using the baseline data. It shows the parameter being predicted, the type of data being used, the set of variables potentially available to the analysis, the variables considered in the analysis, those used in the analysis, the resulting R^2-value, and a commentary on the outcome.

Results showed that temperature can be predicted from sectional data using Vp, dilatation, vertical stress, and lithology with a R^2-value of 0.91. Using resistivity, CSC, and lithology alone, the R^2-value is 0.80.

Lithology can be predicted by considering temperature, Vp, resistivity, CSC, dilatation, and vertical stress but not using temperature and vertical stress in construction of the CART. The R^2-value in this case was 0.82. Removing vertical stress from the analysis results in a R^2-value of 0.53, a 34% decrease in the correlation.

The productive nature of a particular cell using well data can be predicted, considering temperature, Vp, resistivity, CSC, dilatation, the presence of a fault, vertical stress and lithology but not using temperature, dilatation, and the presence of a fault, with a R^2-value of 0.66. When lithology is removed from consideration in the analysis described above, dilatation comes into play, and the resulting R^2-value is 0.52. When Vp, resistivity, the presence of a fault, and lithology are the only parameters considered, all parameters are used except the presence of a fault, and the R^2-value is 0.62. This overall analysis indicated that Vp, resistivity, and lithology alone accounts for 94% of the 0.66 R^2-value described above.

This analysis showed that while CART can determine which parameters would make good predictors, it

also can be used to analyze the complicated relationship between parameters. As in the results of the multi-component, multiple regression analysis, the causal relationships for the interactions found were not explored.

EGS FAVORABILITY/TRUST MAPS

EGS favorability/trust maps were made for the DVGW (i.e., the Calibration Area) at a grid scale of 0.5km by 0.5km for 0.5km incremental horizontal slices between +1km and -4k asl. The three parameters considered most important for EGS are, in order of importance, temperature (above 200°C but less than 350°C), rock type (resistant, competent rock that can form fractures), and stress (extension being more favorable than compression). Since Dixie Valley is located in the B&R, a region of overall extension, we defined four stress sub-parameters to be considered in the favorability/trust analysis (1) fault orientation, (2) presence or absence of a fault, (3) CSC, and (4) occurrence of a structural zone including compression, dilatation, or neither. SMEs were polled to determine the relative favorability values of the individual parameters being considered as well as the final weighting to calculate overall EGS favorability. Final weights for temperature, lithology and stress parameters are 0.51, 0.30 and 0.20, respectively. Table 3 presents the favorability weights and values used. Favorability values were calculated as follows:

$$F_v = (d_0 * w_0) + (d_1 * w_1) + \ldots (d_n * w_n)$$

where F_v is the favorability value for a grid cell, d_0 through d_n is the favorability value of a cell's geoscience parameter data, and w is the weight for a particular data set.

Final baseline EGS favorability maps were calculated and visualized using GIS software (ArcGIS 10). It should be noted that these maps represent one potential realization of the data, albeit, the best one from the authors point of view. A stochastic treatment of the data was not conducted.

Additionally, trust maps were developed to pair with the favorability map to show the reliability of the underlying data. Trust weights range from: hard data (i.e., from wells) with a weight of 5, to modeled data to inferred with weights ranging from 4 to 2 depending on SME confidence in the data, to no data with a weight of 1. The significance of the trust maps has been described in preceding sections. Figure 11 presents the preliminary coupled favorability/trust maps for -1km asl and -2.5km asl. Note that these maps do not account for the presence of non-magnetic Jz rocks observed in the gravity-magnetic models (Plate 1).

Table 2. Preliminary Classification and Regression Tress (CART) Analysis

Description of Analysis Conducted	Data Type	Selected Geoscience Parameters Considered (X) and Used (X) in the Data Splitting Process								r^2-value	Summary
		T [a]	Vp	Resist. (MT)	CSC	Dilat-ation	Fault Presence	Vert Stress [b]	Lith-ology [c,d]		
Predicting Temperature	section	---	X	---	---	X	---	X	X	0.91	
Predicting Temperature		---		X	X	---	---	---	X	0.80	
Predicting Lithology [e]		X	X	X	X	X	---	X	---	0.82	
Predicting Lithology [e]		X	X	X	X	X	---	---	---	0.54	Removing VertStress dropped R^2 value by 34%
Predicting Productive (hydrothermal) Wells for the productive and non-productive well data set	well	X	X	X	X	X	X	X	X	0.66	
		X	X	X	X	X	X	X	---	0.52	R^2-value dropped 21% when Lithology was removed and Dilatation was considered
		---	X	X	---	---	X	---	X	0.62	Vp, MT and Lithology accounts for 94% of the 0.66 r^2-value above
		X	X	X	---	---	X	---	X	0.54	
Predicting Temperature		---	X	---	---	---	---	---	---	0.62	
Predicting Temperature [f]		---	X	---	---	---	---	---	---	0.75	R^2-valued increased by ~21%
Predicting Temperature [f]		---	X	X	---	---	---	---	X	0.75	Adding Resistivity (MT) and Lithology does not change R^2-value relative to using Vp alone
Predicting Temperature [f]		---	X	X	---	---	---	---	---	0.78	Highest R^2 value using Vp and Resistivity (MT)

[a] Temperature

[b] Vertical Stress

[c] Lithologic Density is a parameter that directly reflect the various lithology examined in this investigation

[d] Gravity-magnetic inferred lithology data was found to be highly correlated to lithology and as such is not shown as a separate parameter

[e] Fracture Intensity also considered but not used

[f] Uses all data except wells with low seismic trust (66-21, 45-14, 76-28, 53-15).

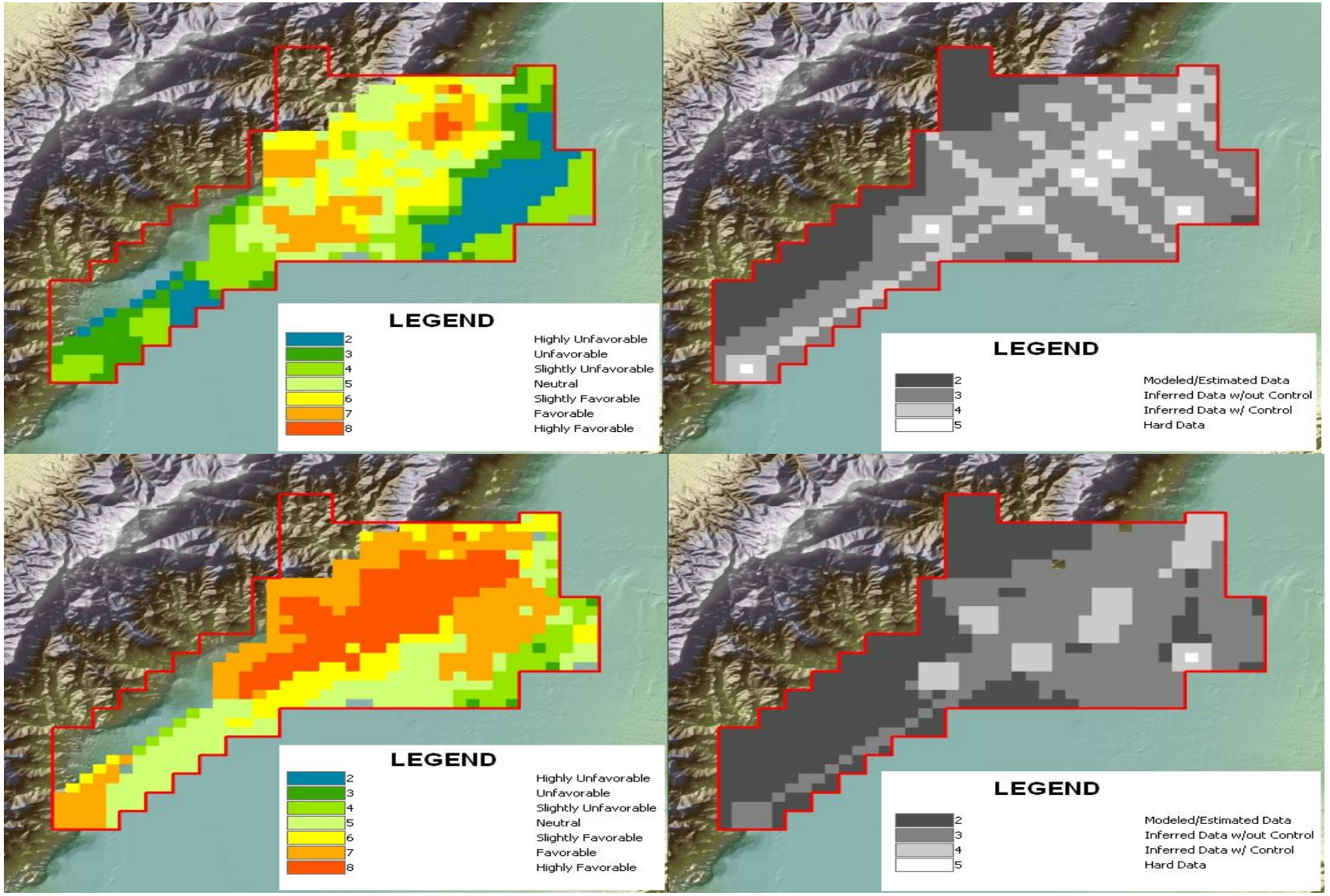

Figure 11: Preliminary EGS favorability maps (left) and associated trust maps (right); see text for an explanation. The upper map (A) is at -1km above sea level or a depth of 2km, while the lower map (B) is at -2.5km above sea level, or a depth of 3.5km. Trust values are presented in shades black and white with the more reliable data cells in a lighter shade.

Table 3. EGS favorability mapping parameters of interest, their values ranging from 1-9 (highlighted in yellow), and weights which sum to 1.

Temp.[1] (0.50 w)		Lithology[2] (0.30 w)		Stress Sub-parameters (.20 w)							
				Compression / Dilation Zone (.05 w)		*Fault Orientation (.05 w)*		*Structure Present (.05 w)*		*Coulomb Stress Change (.05 w)*	
100	1	QTbf	1	Compression	4	30-60°	7	Structure	7	< -22	2
125	2	Tmb	5	Dilation	7	Other	4	None	5	-22	3
150	2	Jz	7	Neither	5	Neither	5			-14	3
175	4	Tr	3							-6	4
200	7	Kgr	9							0	5
225	7	Tv	3							6	6
250	8	Jbr	8							14	7
275	9									22	8
300	8									> 22	9
325	7										
350	5										
> 374	3										

[1] Temperature in °C

[2] Represented by the generalized formations in Dixie Valley

FUTURE WORK

The baseline EDA is being evaluated to determine the precision of the initial findings. This is being accomplished through such techniques as bootstrapping, weighted least squares, and cross-validation. Additionally, a complete sensitivity analysis for the CART analysis will be conducted.

To reduce uncertainty and improve resolution in the geophysical data used in the baseline analysis, we have collected (1) 278 new gravity station measurements, (2) a total of 42 new ambient seismic noise stations under two 21-station three-month campaigns, and (3) 70 MT stations. We have also collected 308 soil CO_2 gas stations to evaluate whether the identified dilation zones are leaking geothermal gases. Figure 12 shows the locations for these new data sets. Finally, both the conductive and convective thermal setting is being modeled. At the time of this writing, all geophysical data is being processed. The soil gas survey did not detect any anomalous CO_2 soil gas except in the immediate vicinity of the fumarolic areas.

The new data will be coupled with the existing data to create an enhanced data set which will be used to generate an enhanced geothermal system model, statistical analysis, and favorability/trust maps.

CONCLUSIONS

A baseline (existing public domain data) conceptual model has been developed for the DVGW. Important results from the baseline assessment are the (1) distinct correlation between the location of shallow thermal anomalies along both sides of the Stillwater Range front and the intersection of north-trending structures with the northeasterly trend of the DVFZ, (2) presence of dilation and compression zones at these structural intersections, (3) the crosscorrelation of production, injection, and dry wells with both the structural zone type in which the well is located and the well's helium R/Ra values, (4) MT anomalous structure in the footwall of the range-front fault component of the DVFZ in the region west of the DVPF (Figure 1) and extending under the eastern portion of the Stillwater Range, and (5) development of supporting data to the identification of the DVFZ postulated by Blackwell et al. (2005). Qualitatively, we have very good correlation among the different geoscience data analyzed. The baseline model data developed is applicable to both to the EGS and hydrothermal components of the Dixie Valley geothermal system.

Initial EDA findings indicated that (1) a statistical relationship can be established between the various geoscience parameters evaluated with high R^2-values for certain predictions and (2) a complex interaction among the various parameter studies is evidenced. These initial findings appear to support the postulation by Biasi et al. (2008) that seismic data can be used to infer temperature.

It is recognized that the data used in the statistical analysis is not an ideal statistical data set because the parameter values used are inferred, modeled, or measured. A fundamental assumption in this analysis is that while the exploration data set is statistically not ideal, and some parameters are more reliable than others, the data can be used to determine statistical significance. The validity of this assumption rests on the notion that whatever uncertainty exists in the different parameters can be thought of as a measurement error, and is at least from a practical standpoint, unbiased. Additionally, the casual reasons for all the identified statistical relationships were not investigated.

Preliminary baseline EGS favorability/trust maps were constructed deterministically by our SMEs. Potential areas of EGS interest were identified based on an integrated assessment of the three EGS parameters of interest: temperature, lithology and stress, (i.e., favorability map) and the reliability of the underlying data defined (i.e., trust map).

Additional statistical work is underway to determine the precision of the analyses performed. New geophysical data sets with increased spatial resolution have been and are being processed.

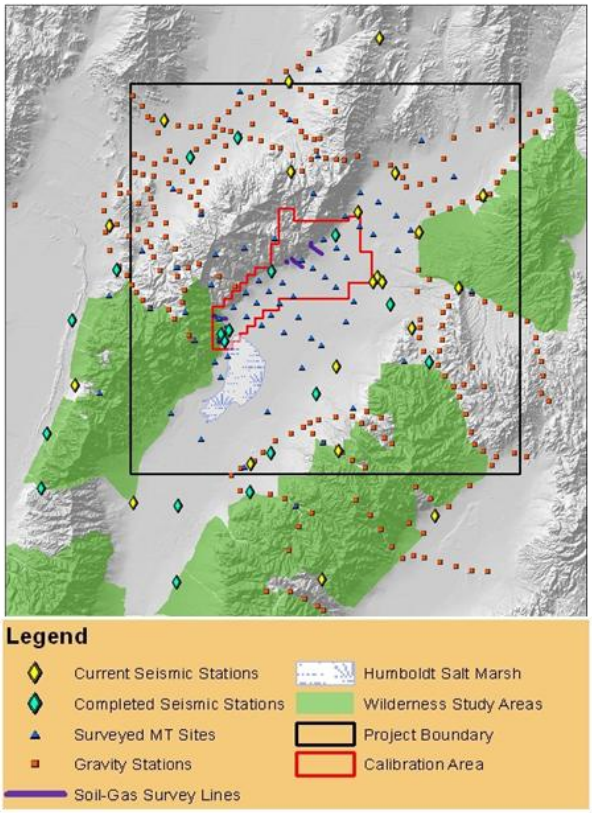

Figure 12: Location of Newly Collected Geoscience Data in 2011-2012. The Project Area is shown as the black bounded box.

REFERENCES

Benoit, D. (1999), "Conceptual Models of the Dixie Valley, Nevada Geothermal Field," *Geothermal Resources Council (GRC) Transactions*, **23**, Oct. 17-20.

Biasi, G., Tibuleac, I., and Preston, L. (2008), "Regional resource area mapping in Nevada using the USArray Seismic Network," paper presented at the *Geothermal Energy 2008 Conference and Expo*, Reno, NV, Oct 5-8.

Blackwell, D.D., Smith, R.P., Waibel, A. F., Richards, M.C., Stepp, P. (2009), "Why Basin and Range Systems are Hard to Find II: Structural Model of the Producing Geothermal System in Dixie Valley, Nevada," *GRC Transactions*, **33**, 441-446. Blackwell, D. D., Smith, R. P., and Richards, M. (2007). "Exploration and Development at Dixie Valley, Nevada: Summary of DOE Studies," *Proceedings, **32nd** Workshop on Geothermal Reservoir Engineering*, Stanford University, California, Jan. 22-24, 16 p.

Blackwell D.D., Smith R.P., Editors. Bergman, S., Blackwell, D.D., Goff, F. Kennedy, B.M., McKenna, J.R., Richards, M. C., Smith, R.P., Waibel, A.F., Wannamaker, P. E. (2005), "Description, Synthesis, and Interpretation of the Thermal Regime, Geology, Geochemistry and Geophysics of the Dixie Valley, Nevada Geothermal System," (*unpublished DRAFT DOE Technical Report*), 195 p.

Caskey, S.J., Wesnousky, S.G. (2000), "Active Faulting and Stress Redistributions in the Dixie Valley, Beowawe, and Bradys Geothermal Fields: Implications for Geothermal Exploration in the Basin and Range," *Proceedings, **25th** Workshop on Geothermal Reservoir Engineering*, Stanford University, California, Jan. 24-26, 16 p.

Caskey, S.J, Wesnousky, S.G., Zhang, P., and Slemmons, D.B. (1996). "Surface Faulting of the 1954 Fairview Peak (M_s7.2) and Dixie Valley (M_s6.8) Earthquakes, Central Nevada," Bull. Seismological Society of America, **86**, 3, 761-787.

Goff, F., Bergfeld, D., Janik, C.J., Counce, D., and Murrell, M. (2002). "Geochemical data on waters, gases, scales, and rocks from the Dixie Valley region, Nevada (1996-1999)," Los Alamos National Laboratory. *Report LA-13972-MS*, 71 p.

Grauch, V.J.S. (2002),"High-resolution aeromagnetic survey to image shallow faults, Dixie Valley geothermal field, Nevada," U.S. Geological Survey Open-File Report 02-0384, available on-line at *http://pubs.usgs.gov/of/2002/ofr-02-0384/*.

Hickman, S.H., Zoback, M.D., Barton, C.A., Benoit, R., Svitek, J., Summers, R. (2000), "Stress and Permeability Heterogeneity within the Dixie Valley Geothermal Reservoir: Recent Results from Well 82-5," *Proceedings, 25th Workshop on Geothermal Reservoir Engineering*, Stanford University, California, Jan. 24-26, 10 p.

Hickman, S., Zoback, M., Benoit, R. (1998), "Subsurface Electrical Measurements at Dixie Valley, Nevada, Using Single-Well and Surface-to-Well Induction Logging," *Proceedings, 23rd Workshop on Geothermal Reservoir Engineering*, Stanford University, California, Jan. 26-28, 8 p.

Iovenitti J.L., Blackwell, D.D., Sainsbury, J.S., Tibuleac, I.M., Waibel, A.F., Cladouhos, T.T., Karlin, R., Kennedy, B.M., Isaaks, E., Wannamaker P.E., Clyne, M.T., Callahan, O.C. (2011a), "EGS Exploration Methodology Development Using the Dixie Valley Geothermal District as a Calibration Site, A Progress Report," *GRC Transactions*, **35**, 12 p.

Iovenitti J.L., Blackwell, D.D., Sainsbury, J.S., Tibuleac, I.M., Waibel, A.F., Cladouhos, T.T., Karlin, R., Kennedy, B.M., Isaaks, E., Wannamaker P.E., Clyne, M.T., Callahan, O.C. (2011b), "EGS Exploration Methodology Development Using the Dixie Valley Geothermal District as a Calibration Site, A Progress Report," *Poster Presentation, Annual GRC Meeting in San Diego*.

Kennedy, B.M., van Soest, M.C. (2006), "A Helium Isotope Perspective on the Dixie Valley, Nevada, Hydrothermal System," *Geothermics*, **35**, 26-43 p.

Lawrence, R. L., Wright, A. (2001), "Rule-Based Classification Systems using Classification and Regression (CART) Analysis," *Photogrammetric Engineering & Remote Sensing*, **67**, No. 10, 1137-1142 p.

Lutz, S.J., Moore, J.N., Benoit, D. (1997), "Geologic Framework of Jurassic Reservoir Rocks in the Dixie Valley Geothermal Field, Nevada: Implications from Hydrothermal Alteration and Stratigraphy," *Proceedings, 22nd Workshop on Geothermal Reservoir Engineering*, Stanford University, California, Jan. 27-29, 9 p.

Okaya, D.A., and Thompson, G.A. (1985), "Geometry of Cenozoic extensional faulting: Dixie Valley, Nevada," *Tectonics*, **4** (1), 107-125.

Page, B.M. (1965), "Preliminary Geologic Map of a part of the Stillwater Range, Churchill County, Nevada," *Nevada Bureau of Mines*, Map 28.

Ponce, D. A. (1997), "Gravity data of Nevada," U.S. Geological Survey Digital Data Series DDS-41, 1-27.

Reed, M.J. (2007), "An Investigation of the Dixie Valley Geothermal Field, Nevada, Using Temporal Moment Analysis of Tracer Tests," *Proceedings, 32nd Workshop on Geothermal Reservoir Engineering*, Stanford University, California, Jan. 22-24, 8 p.

Smith, R.P., Grauch, V.J.S., and Blackwell, D.D. (2002), "Preliminary Results of a High-Resolution Aeromagnetic Survey to Identify Buried Faults at Dixie Valley, Nevada," *GRC Transactions*, **26**, 543-546.

Smith, R. P.,Wisian K. W., and Blackwell, D.D. (2001), "Geological and geophysical evidence for intra-basin and footwall faulting at Dixie Valley, Nevada," *GRC Transactions*, **25**, 323-326.

Speed, R.C. (1967), "Geologic Map of the Humboldt Lopolith and surrounding terrane," *The Geologic Society of America, Inc., Map and Chart* Series MC-14. *4 p.*

Stewart, J.H., and Carlson, J.E. (1978), "Geologic map of Nevada", *U.S. Geological Survey*, 1:500,000 scale.

Tibuleac I.M., Von Seggern D.H., Louie J.N., and Anderson J.G. (2009), "High Resolution Seismic Velocity Structure in the Reno Basin from Ambient Noise Recorded by a Variety of Seismic Instruments," *GRC Transactions*, **33**, 143-146.

Waibel, A.F. (1987), "An Overview of the Geology and Secondary Mineralogy of the High Temperature Geothermal Systems in Dixie Valley, Nevada," *GRC Transactions*, **11**, 479-486, and *GRC Bulletin*, **16**(9), 5-13.

Waibel, A.F. (2011), "Structural controls on the location of geothermal cells in and adjacent to Dixie Valley, Nevada," *GRC Transactions*, **35**, 8 p.

Wallace R. and Whitney R. (1984), "Late quaternary history of the Stillwater seismic gap, Nevada," *Bulletin of the Seismological Society of America*, **74**(1), February, 301-314.

Wannamaker P.E., Doerner, W.M., and Hasterok D.P. (2007), "Integrated Dense Array and Transect MT Surveying at Dixie Valley Geothermal Area, Nevada; Structural Controls, Hydrothermal Alteration and Deep Fluid Sources," *Proceedings 32nd Workshop on Geothermal Reservoir Engineering*, Stanford University, California, Jan. 22-24, 6 p.

Wannamaker P.E., Doerner W.M., and Hasterok D.P. (2006), "Cryptic Faulting and Multi-Scale Geothermal Fluid Connections in the Dixie Valley-Central Nevada Seismic Belt Area; Implications from MT Resistivity Surveying," *Proceedings 31st Workshop on Geothermal Reservoir Engineering*, Stanford University, California, Jan. 30-Feb. 1, 8 p.